Обзор ArXiv/astro-ph, 31 мая – 4 июня 2021

От Сильченко О.К.

ArXiv: 2105.13684

Dark Matter Fraction in $z \sim 1$ Star-Forming Galaxies

Gauri Sharma,[1,2,3,⋆] Paolo Salucci[1,2,3] and Glenn van de Ven[4]

[1] SISSA International School for Advanced Studies, Via Bonomea 265, I-34136 Trieste, Italy
[2] GSKY, INFN-Sezione di Trieste, via Valerio 2, I-34127 Trieste, Italy
[3] IFPU Institute for Fundamental Physics of the Universe, Via Beirut, 2, 34151 Trieste, Italy
[4] Department of Astrophysics, University of Vienna, Türkenschanzstrasse 17, 1180 Wien, Austria

Received 11/02/2021; accepted 27/05/2021

ABSTRACT

Context. The study of dark matter (DM) across the cosmic time-scales is essential for understanding the galaxy formation and evolution. Recent observational studies show that the further back in time ($z > 0.5$), rotation-supported star-forming galaxies (SFGs) begin to appear dark matter deficient compared to local SFGs.

Aims. We present a observational study of the dark matter fraction in 225 rotation supported star-forming galaxies at $z \approx 0.9$ having stellar mass range: $9.0 \leq log(M_* \, \mathrm{M}_\odot) \leq 11.0$ and star formation rate: $0.49 \leq log\left(SFR \, [\mathrm{M}_\odot \, \mathrm{yr}^{-1}]\right) \leq 1.77$.

Methods. We study a sub-sample of the KMOS redshift one spectroscopic survey (KROSS) studied by Sharma et al. (2021). The stellar masses (M_*) of these objects were previously estimated using mass-to-light ratios derived from fitting the spectral energy distribution of the galaxies. Star formation rates were derived from the H_α luminosities. The total gas masses (M_{gas}) are determined by scaling relations of molecular and atomic gas (Tacconi et al. 2018; Lagos et al. 2011, respectively). The dynamical masses (M_{dyn}) are directly derived from the rotation curves (RCs) at different scale lengths (effective radius: R_e, $\sim 2\,R_e$ and $\sim 3\,R_e$) and then the dark matter fractions ($f_{DM} = 1 - M_{bar}/M_{dyn}$) at these radii are calculated.

Results. We report that at $z \sim 1$ only a small fraction ($\sim 5\%$) of our sample has a low ($< 20\%$) DM fraction within $\sim$ 2-3 R_e. The majority ($> 72\%$) of SFGs in our sample have dark matter dominated outer disks ($\sim 5 - 10$ kpc) in agreement with local SFGs. Moreover, we find a large scatter in the fraction of dark matter at a given stellar mass (or circular velocity) with respect to local SFGs,

CROSS(z=1)+3DBarolo

tional to the stellar Freeman disk length R_D[5] (Freeman 1970), for example $R_e = 1.69\ R_D$. Under the same assumption, the optical radius R_{opt} containing 83% of the integrated light becomes $R_{opt} = 3.2\ R_D$. In the Q12 sample, the median effective radius is $\sim$ 3.1 kpc and the median optical radius is $\sim$ 5.9 kpc. This means that the effective radius of the majority of the sample falls below the resolution limit ($\sim$ 4.0 kpc, since the median seeing is 0.5″ at $z \sim 0.9$), while the optical radius is of the same order. Therefore, to be conservative and trace the DM fraction to the furthest point where we have data, we define the outer radius $R_{out} = 5\ R_D$, which stays above the resolution limit in majority ($\approx$ 99%) of the sample.[6]

Furthermore, for sample's accuracy and quality, we remove galaxies those have $R_{out} < 3.5$ kpc (below the resolution limit), $z < 0.65$, and $M_* < 10^9 M_\odot$,[7] in total we removed 31 galaxies. Our final sample contains 225 galaxies that have the inclination range: $25° < \theta_i \leq 75°$, the redshift range: $0.76 \leq z \leq 1.04$, the effective radii: $0.08 \leq \log(R_e\ [\mathrm{kpc}]) \leq 0.89$, and the circular velocities: $1.45 \leq \log(V_{out}\ [\mathrm{km\ s^{-1}}]) \leq 2.83$, where V_{out} is calculated at R_{out}.

Замах на 4 разных радиуса

Содержание барионов

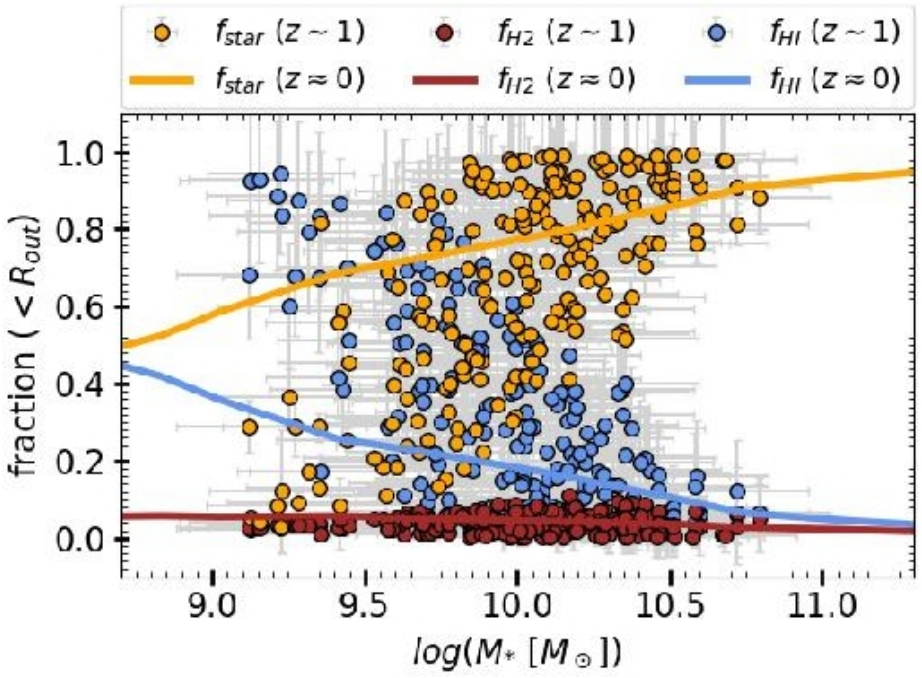

- Звездная масса M_*: из M_H, fix M/L_H=0.2
- Масса молекулярного газа: scaling relation vs (1+z), M_*, отход от главной послед.
- Масса атомарного газа: scaling relation vs M(H_2), (1+z), M_*
- Распределение по радиусу – exp с масштабом по ионизованному газу

Есть скрытая масса!

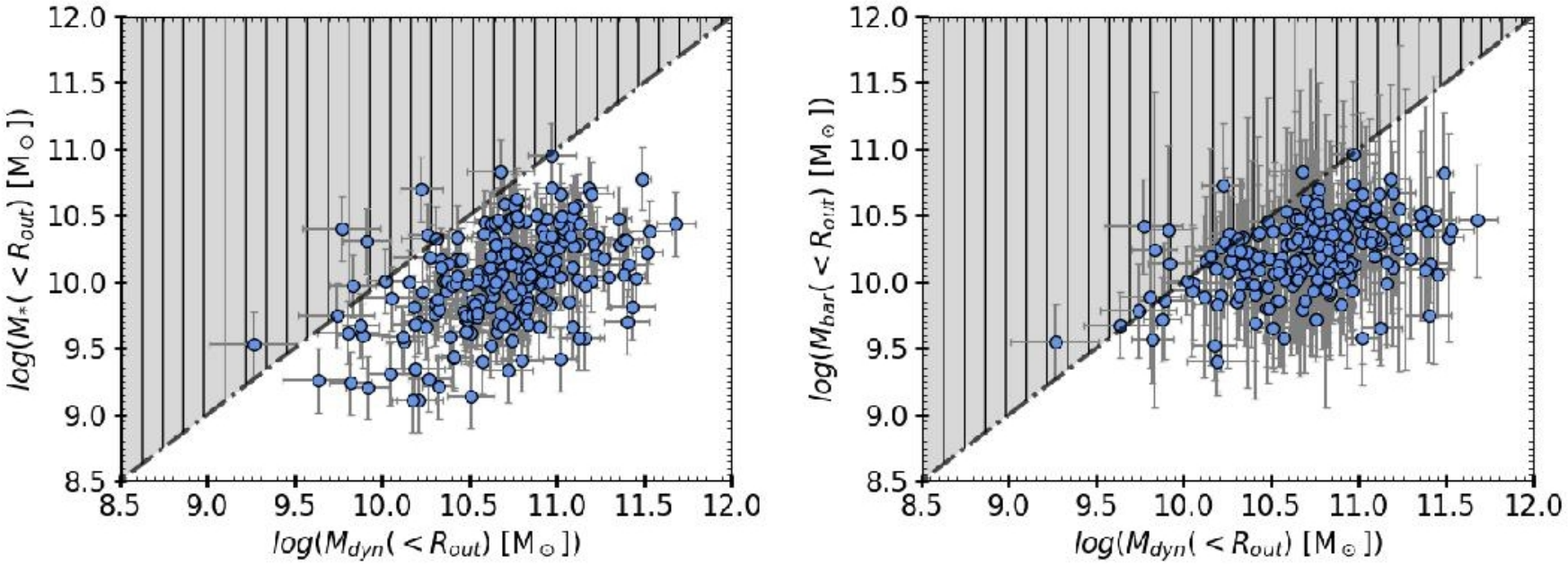

Fig. 2. The stellar and baryonic masses as a function of dynamical mass (left and right panels, respectively), computed within R_{out}. The notations and color codes are the same in both panels and are given as follows: The filled blue circles represent the data, the black dotted dashed line shows the one-to-one plane, and the grey hatched-shaded area represents the forbidden region.

Тренды и сравнение с локальной Вселенной на разных радиусах

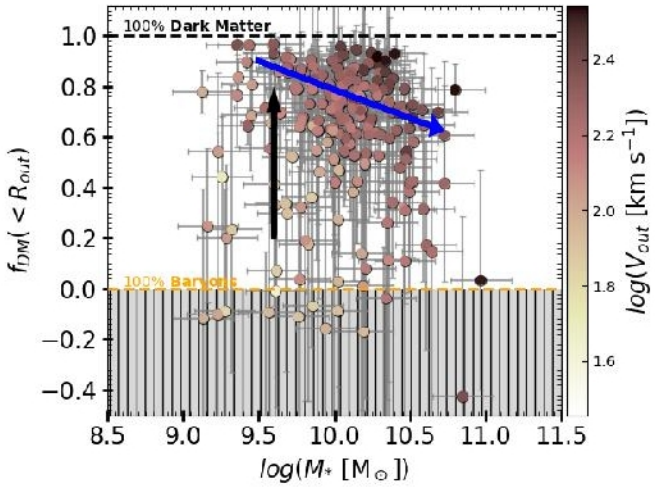

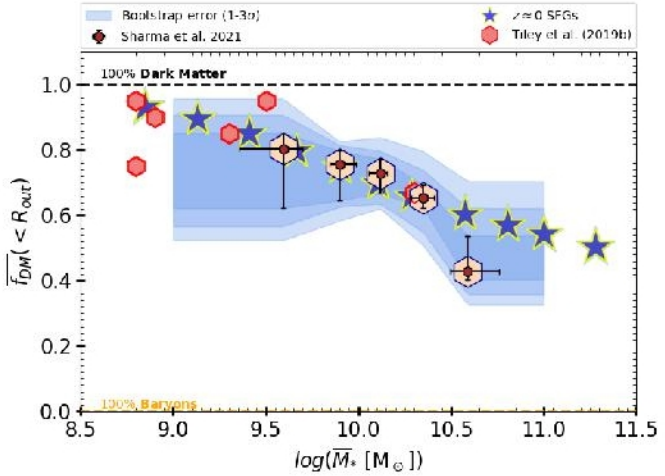

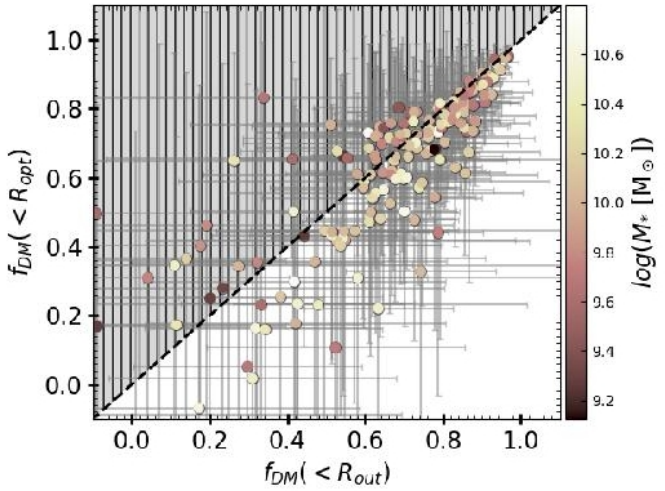

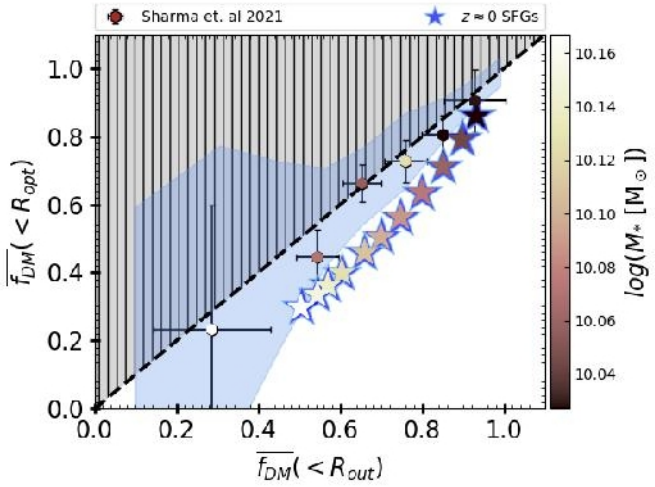

Вообще-то, расхождения с Генцелем нет…

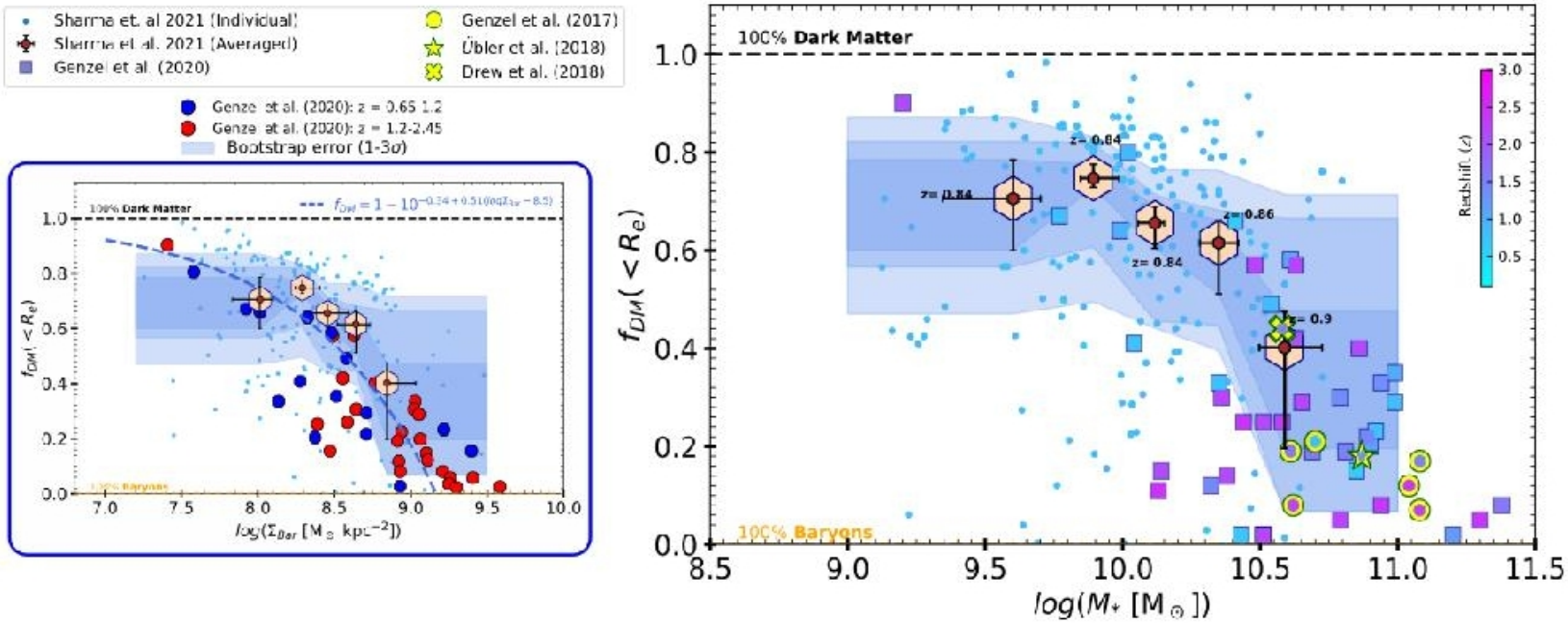

Fig. 5. Comparison of averaged DM fraction (within R_e) of our sample with previous high-z studies. *Left panel:* dark matter fraction as a function of baryon surface density $\Sigma_{Bar}(< R_e) = M_{bar}(< R_e)/\pi R_e^2$. The brown hexagons with errorbars shielded by big light-peach hexagons are our averaged dataset, and individual galaxies are shown by small dots, color-coded by redshift. The blue shaded area represents the $1-3\sigma$ error on DM fraction. The blue dashed line shows the relation $f_{DM}(< R_e) = 1 - 10^{-0.34+0.51(log\Sigma_{Bar}-8.5)}$ given by Genzel et al. (2020) and their data is plotted in blue ($z = 0.65-1.2$) and red ($z = 1.2-2.45$) filled circles. *Right panel:* dark matter fraction as a function of stellar mass, color-coded by redshit. Our dataset and its errors are presented in similar manner in both panels. Genzel et al. (2020) data is shown by filled squares. The measurements of Genzel et al. (2017), Drew et al. (2018) and Übler et al. (2018) are shown by yellow circles, star and cross, respectively, where interior of each marker is color-coded by redshift. Notice, legend of the right plot is shown at the top of left plot.

ArXiv: 2106.01928

The SAMI Galaxy Survey: Trends in $[\alpha/\mathrm{Fe}]$ as a Function of Morphology and Environment

Peter J. Watson,[1★] Roger L. Davies,[1] Sarah Brough,[2,3] Scott M. Croom,[2,4] Francesco D'Eugenio,[5] Karl Glazebrook,[2,6] Brent Groves,[7] Ángel R. López-Sánchez,[2,8,9] Jesse van de Sande,[2,4] Nicholas Scott,[2,4] Sam P. Vaughan,[4] Jakob Walcher,[10] Joss Bland-Hawthorn,[4] Julia J. Bryant,[2,4,11] Michael Goodwin,[8] Jon S. Lawrence,[12] Nuria P. F. Lorente,[8] Matt S. Owers,[2,9,13] and Samuel Richards[14]

[1] *Sub-Department of Astrophysics, Department of Physics, University of Oxford, Denys Wilkinson Building, Keble Rd., Oxford OX1 3RH, UK*
[2] *ARC Centre of Excellence for All Sky Astrophysics in 3 Dimensions (ASTRO 3D)*
[3] *School of Physics, University of New South Wales, NSW 2052, Australia*
[4] *Sydney Institute for Astronomy (SIfA), School of Physics, University of Sydney, NSW 2006, Australia*
[5] *Sterrenkundig Observatorium, Universiteit Gent, Krijgslaan 281 S9, B-9000 Gent, Belgium*
[6] *Centre for Astrophysics & Supercomputing, Swinburne University of Technology, Victoria 3122, Australia*
[7] *Research School of Astronomy & Astrophysics, Australian National University, Mt Stromlo Observatory, Cotter Rd, Weston Creek, ACT 2611, Australia*
[8] *Australian Astronomical Optics, Macquarie University, 105 Delhi Rd, North Ryde, NSW 2113, Australia*
[9] *Department of Physics and Astronomy, Macquarie University, NSW 2109, Australia*
[10] *Leibniz-Institut für Astrophysik Potsdam (AIP), An der Sternwarte 16, D-14482 Potsdam, Germany*
[11] *Australian Astronomical Optics, AAO-USydney, School of Physics, Building A28, University of Sydney, NSW 2006, Australia*
[12] *Australian Astronomical Optics - Macquarie, Macquarie University, NSW 2109, Australia*
[13] *Astronomy, Astrophysics and Astrophotonics Research Centre, Macquarie University, Sydney, NSW 2109, Australia*
[14] *SOFIA Science Center, USRA, NASA Ames Research Center, Building N232, M/S 232-12, P.O. Box 1, Moffett Field, CA 94035-0001, USA*

Выборка: SAMI, третий релиз

2.1 SAMI Galaxy Survey

The SAMI instrument and survey design are detailed extensively in both Croom et al. (2012) and Bryant et al. (2015). The instrument comprises 13 IFUs (the *hexabundles*), which can be deployed over a 1-degree diameter field of view, each with an individual field of view of 15 arcsec (Bland-Hawthorn et al. 2011; Bryant et al. 2014). The IFUs are mounted at the prime focus of the Anglo-Australian Telescope (AAT), and each consists of 61 individual fibres. Observations are dithered to create data cubes with a 0.5-arcsec spaxel size. All 819 fibres (including 26 allocated to blank sky observations for calibration purposes) are fed into the AAOmega spectrograph (Saunders et al. 2004; Smith et al. 2004; Sharp et al. 2006). This is composed of a blue arm, with spectral resolution $R \sim 1800$ over the wavelength range 3750-5750 Å, and a higher resolution red arm, with wavelength coverage 6300-7400 Å and $R \sim 4300$ (van de Sande et al. 2017).

The SGS consists of 3426 observations of 3068 unique galaxies, available as part of public Data Release 3 (Croom et al. 2021). The survey spans a redshift range $0.004 < z < 0.115$, and a stellar mass range $M_* \sim 10^7$ to $10^{12}\ M_\odot$. Field and group galaxies were drawn from the Galaxy And Mass Assembly (GAMA) survey (Driver et al. 2011), with the selection being volume-limited in each of four stellar mass cuts. An additional sample of cluster galaxies was drawn from the survey of eight low-redshift clusters in Owers et al. (2017), to extend the environmental sampling.

- Ликские индексы, SSP, модель подгоняют ПО ВСЕМ ИНДЕКСАМ
- Модели Томаса и др.
- ВЫКИНУТЫ все галактики, которые ушли за пределы моделей
- Ограничение z<0.07
- Ограничение σ >40км/с

Почистили-почистили выборку, поделили по типами и синие-красные

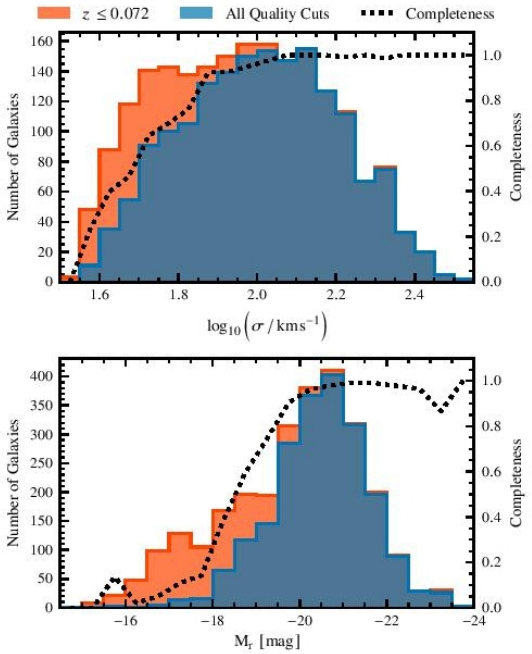

Sample	Total	Optical Morphology					Section
		E	S0	Sa/b	Sc	Unclassified	
All Observations	3426	603	785	682	1182	174	
Unique Galaxies	3068	561	728	605	1026	148	
$z \leq 0.072$	2773	459	630	544	1002	138	B1
Quality Cuts	2093	453	623	524	404	89	3.6
$\log_{10}(\Sigma_5) \leq 1.15$	1416	216	363	424	362	51	4
$\log_{10}(\Sigma_5) > 1.15$	660	230	252	95	46	37	4
		Early Type Galaxies					
		E		E/S0		S0	
$\log_{10}(\Sigma_5) \leq 1.15$	379	111		104		164	4
$\log_{10}(\Sigma_5) > 1.15$	375	130		99		146	4

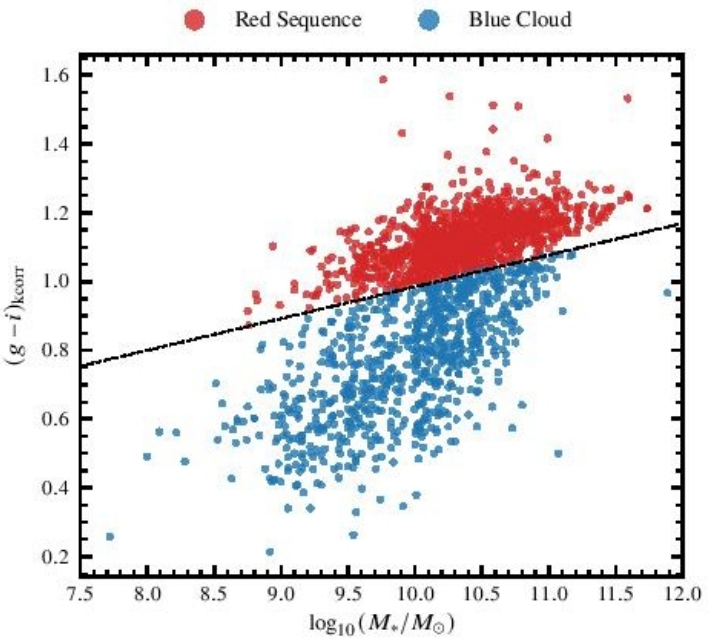

Figure 4. The distribution of k-corrected $(g-i)$ galaxy colours as a function of stellar mass, for our final sample. The dividing line between the red sequence and blue cloud is taken from Owers et al. (2017).

Еще разделили по плотности окружения

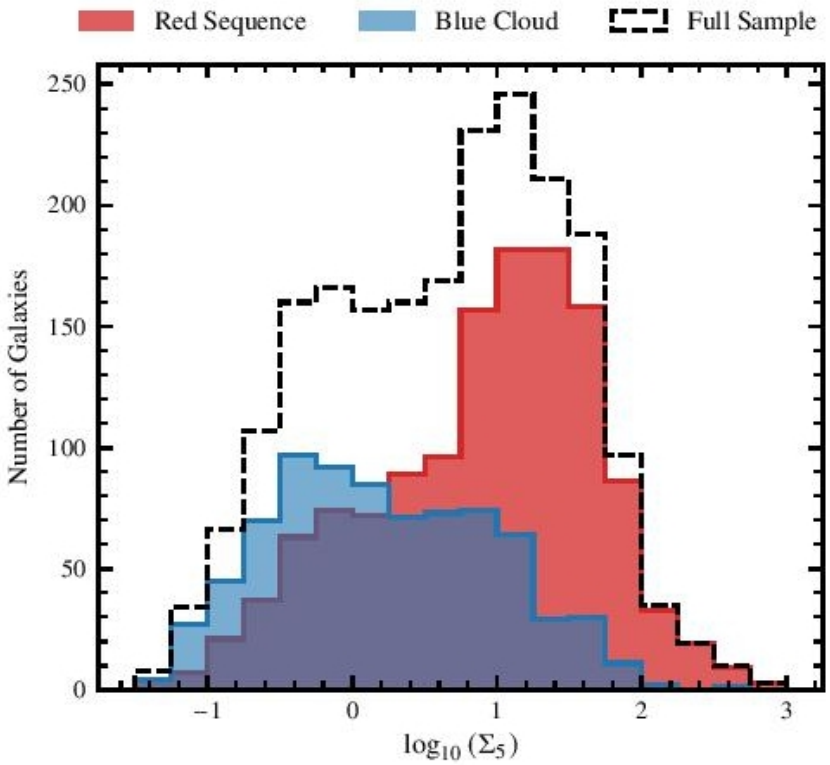

Figure 5. The distribution of $\log_{10}(\Sigma_5)$ for red sequence and blue cloud galaxies, alongside the full sample. At the highest values of $\log_{10}(\Sigma_5)$, galaxies almost exclusively belong to the red sequence, whereas we find a more balanced distribution towards lower values of $\log_{10}(\Sigma_5)$.

От чего смотреть отскок? И как учесть density-morph. Type?

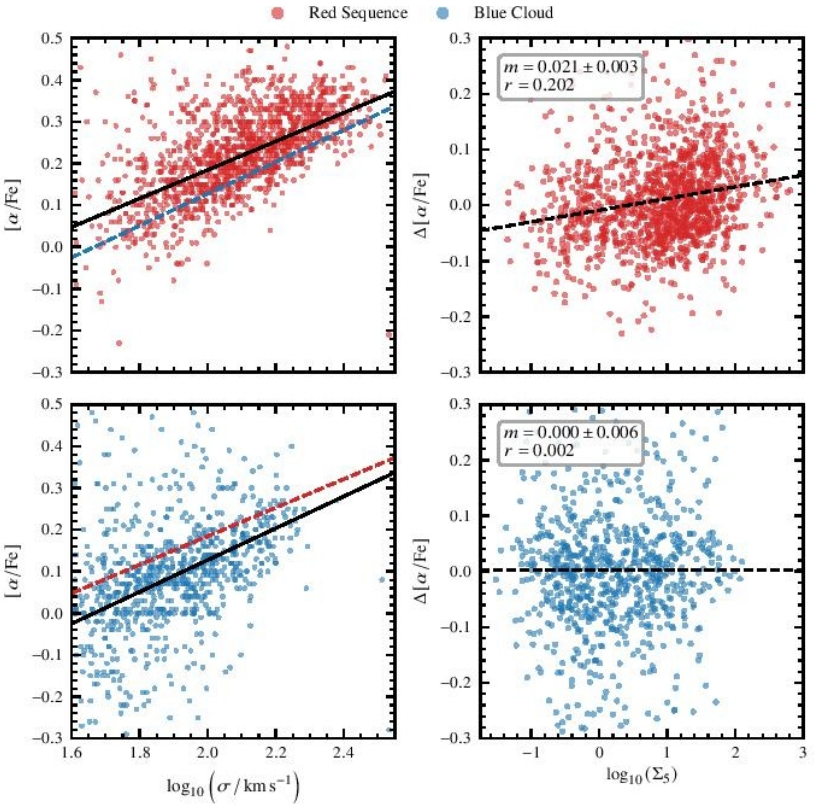

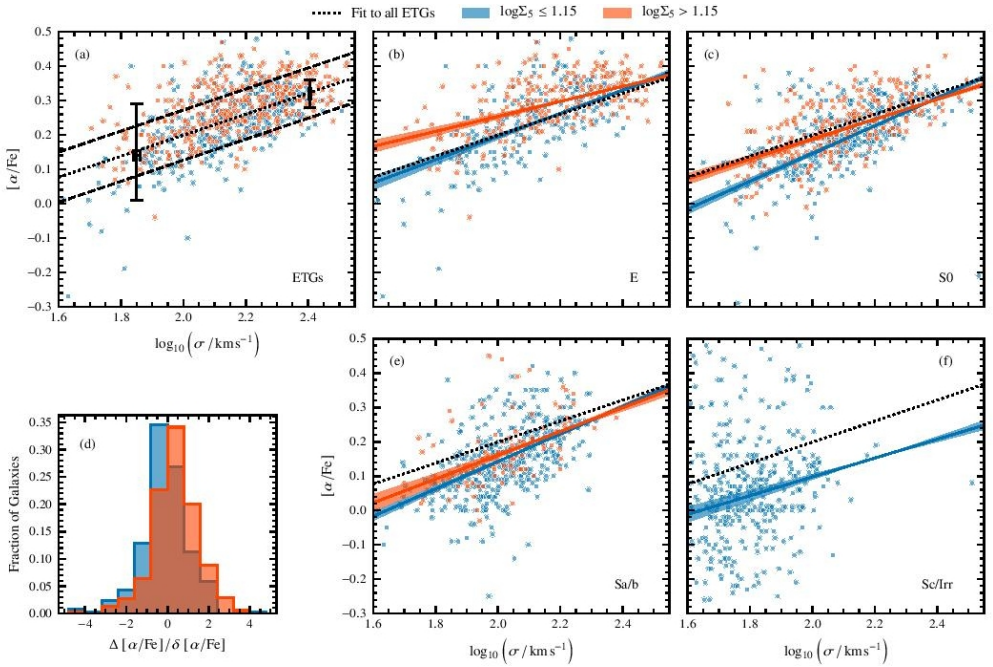

Плотность окружения влияет!

Собственно, окружение влияет только на маломассивные галактики

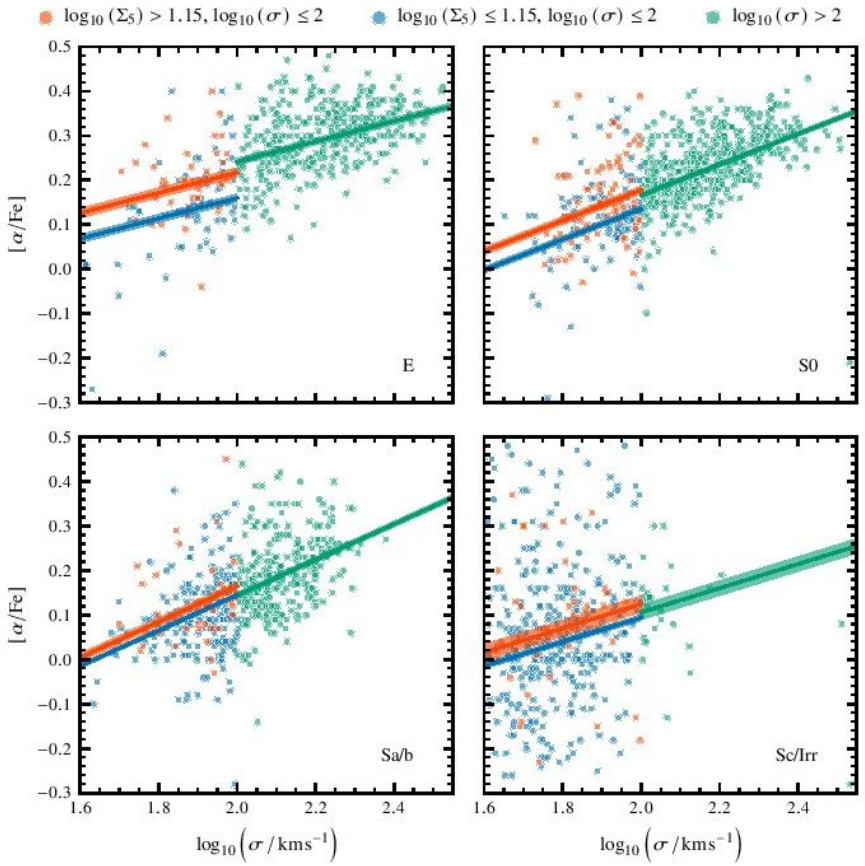

Figure 8. For each morphology, we fit linear trendlines to all galaxies above $\log_{10}(\sigma) > 2$. We then fit each environment separately for $\log_{10}(\sigma) \leq 2$, fixing the gradient to the value measured at higher σ.

А вот так вроде и на средние тоже…

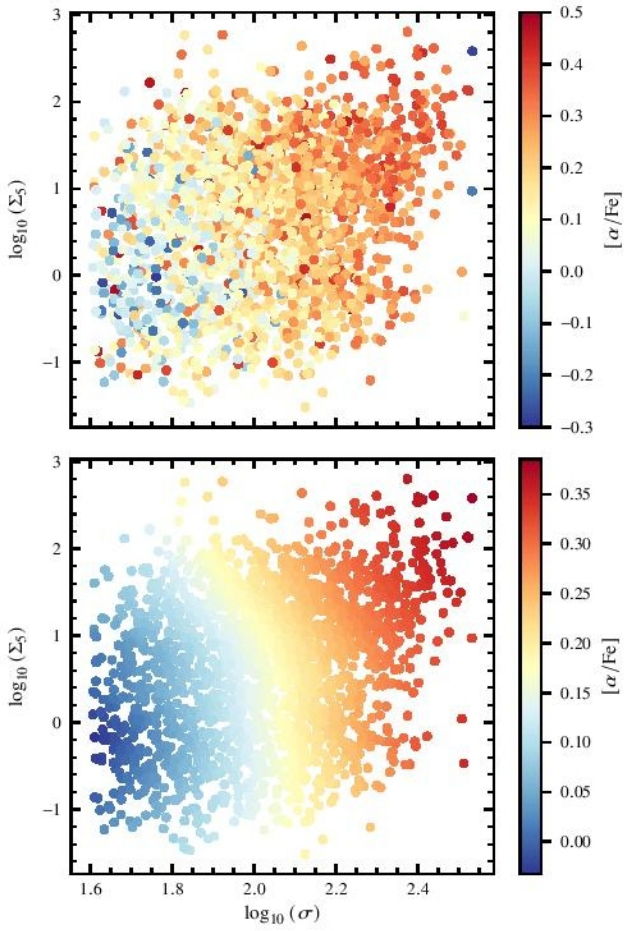

Выводы сделаны достаточно аккуратно:

- Зависимость [α/Fe] от плотности окружения есть только для красных галактик.
- Значимое отличие, +0.06 dex, зафиксировано только для карликовых галактик, σ<100 км/с
- Отличие сильнее для эллиптических, чем для спиральных – 4σ против 2σ
- Внутри плотного окружения работает морфологический фактор: эллиптические галактики на 0.1dex обогащеннее альфа-элементами, чем дисковые